High efficiency of livestock ammonia emission controls on alleviating particulate nitrate during a severe winter haze episode in northern China

Zhenying Xu[1], Mingxu Liu[1], Minsi Zhang[2], Yu Song[1*], Shuxiao Wang[3*], Lin Zhang[4], Tingting Xu[1], Tiantian Wang[1], Caiqing Yan[1], Tian Zhou[1], Yele Sun[5], Yuepeng Pan[5], Min Hu[1], Mei Zheng[1*] and Tong Zhu[1]

[1]State Key Joint Laboratory of Environmental Simulation and Pollution Control, Department of Environmental Science, Peking University, Beijing, 100871, China

[2]National Center for Climate Change Strategy and International Cooperation (NCSC)

[3]State Key Joint Laboratory of Environment Simulation and Pollution Control, School of Environment, Tsinghua University, Beijing 100084, China

[4]Laboratory for Climate and Ocean-Atmosphere Studies, Department of Atmospheric and Oceanic Sciences, School of Physics, Peking University, Beijing 100871, China

[5]State Key Laboratory of Atmospheric Boundary Layer Physics and Atmospheric Chemistry, Institute of Atmospheric Physics, Chinese Academy of Sciences, Beijing 100029, China

[*]Corresponding author: Yu Song (songyu@pku.edu.cn), Shuxiao Wang (shxwang@tsinghua.edu.cn), Mei Zheng (mzheng@pku.edu.cn).

31

Abstract

Although nitrogen oxide (NO_x) emission controls have been implemented for several years, northern China is still facing high particulate nitrate (NO_3^-) pollution during severe haze events in winter. In this study, the thermodynamic equilibrium model (ISORROPIA-II) and the Weather Research and Forecast model coupled chemistry (WRF-Chem) were used to study the efficiency of NH_3 emission controls on alleviating particulate NO_3^- during a severe winter haze episode. We found that particulate NO_3^- formation in extremely high pollution is almost NH_3-limited, not NO_x-limited often happened in the other days. The improvements in manure management of livestock husbandry could reduce 40% of total NH_3 emissions (currently 100 kiloton per a month) in winter of northern China. Consequently, particulate NO_3^- was reduced by approximately 40% (averagely from 40.8 to 25.7 $\mu g/m^3$). Our results indicate that reducing livestock NH_3 emissions would be highly effective to reduce particulate NO_3^- during severe winter haze events.

1 Introduction

In northern China (including Beijing, Tianjin, Hebei, Shandong, Shanxi and Henan), severe haze pollution events occur frequently during wintertime, with the concentration of $PM_{2.5}$ (particles with an aerodynamic diameter less than 2.5 μm) reaching hundreds of micrograms per cubic meter and SIA (secondary inorganic aerosol) accounting for more than 50% of $PM_{2.5}$ (Zheng et al., 2016;Tan et al., 2018). To mitigate fine particle pollution, the Chinese government has been taking strong measures to control SO_2 emissions (http://www.gov.cn/zwgk/2011-12/20/content_2024895.htm). Since 2007, SO_2 emissions have been reduced by 75% in China (Li et al., 2017). Consequently, the particulate sulfate concentration has also been declining continuously in the past decade (Geng et al., 2017).

Although NO_x emissions in 48 Chinese cities decreased by 21% from 2011 to 2015 (Liu et al., 2017a), unfortunately, no obvious decreasing trend for particulate NO_3^- had been observed in northern China during recent years (Zhang et al., 2015). In October 2015, a severe haze episode was reported in North China Plain (NCP), with the hourly peak concentration of particulate NO_3^- exceeding 70 μg/m^3 (Zhang et al., 2018b). Even in November 2018, during a heavy haze episode in northern China, the hourly peak concentration of $PM_{2.5}$ still exceeded 289 μg/m^3, of which particulate NO_3^- accounted for 30% (http://www.mee.gov.cn/xxgk2018/xxgk/xxgk15/201811/t20181116_674022.html).

Another way to alleviate the particulate NO_3^- pollution is to control NH_3 emissions. Previous studies were performed to demonstrate the necessity of NH_3 emissions abatement in reducing $PM_{2.5}$ concentrations in the United States (Pinder et al., 2007;Tsimpidi et al., 2007;Pinder et al., 2008;Wu et al., 2016) and Europe (de Meij et al., 2009;Bessagnet et al., 2014;Backes et al., 2016). Recently, a feature article pointed out that NH_3 could be key to limiting particulate pollution (Plautz, 2018). In contrast with low particulate matter pollution levels in the United States and Europe, what we are facing in northern China is the extremely high particulate NO_3^- pollution especially happened in severe winter haze

73 events.

74   Although Fu et al. (2017) proposed that the NH_3 emission controls are urgently
75 required in China, the effectiveness of NH_3 emissions mitigation to alleviate the particulate
76 NO_3^- peaks during severe winter haze episodes was seldom reported. Only Guo et al.
77 (2018b) used a thermodynamic model to estimate the sensitivity of particulate NO_3^- to TA
78 (sum of ammonia and ammonium) during one winter haze episode in Beijing. In their study,
79 the atmospheric chemistry simulations based on NH_3 emission controls scenario were
80 lacking to demonstrate the regional effects.

81   To alleviate severe particulate NO_3^- pollution in northern China is urgent, the study on
82 the effectiveness by NH_3 emission controls is necessary. In this study, we firstly compile a
83 comprehensive NH_3 emission inventory for northern China in winter of 2015, and estimate
84 the NH_3 emission reductions by improving manure management. Then, the ISORROPIA-
85 II and WRF-Chem models are used to investigate the effectiveness of NH_3 emission
86 reductions on alleviating particulate NO_3^- during a severe haze episode. The molar ratio
87 based on observations is used to explore the efficiency of particulate NO_3^- reductions
88 during the severe haze conditions in wintertime.

89

2 Methods and Materials

2.1 Observational data

92   Hourly time-resolution aerosol and gas measurements were conducted at the Peking
93 University urban atmosphere environment monitoring station (PKUERS) (39.991N,
94 116.313E) in Beijing in December 2015 and December 2016. A commercialized semi-
95 continuous In-situ Gas and Aerosol Composition (IGAC) Monitor was used to measure the
96 concentrations of water-soluble ions (e.g., NH_4^+, SO_4^{2-}, NO_3^-, Na^+, K^+, Ca^{2+}, Mg^{2+}, Cl^-) in
97 $PM_{2.5}$ and inorganic gases (e.g., NH_3, HNO_3, HCl). Relative humidity (RH) and
98 temperature were observed at 1-min resolution at the same site. The quality assurance and
99 control for the IGAC was described in Liu et al. (2017b). A typical severe haze episode
100 occurred during the 6 to 10 in December 2015, with daily average concentrations of $PM_{2.5}$
101 exceeding 150 μg/m^3 for three days ($PM_{2.5}$ data are from China National Environmental
102 Monitoring Centre). The average RH and temperature in this haze event were $60.9 \pm 11.4\%$
103 and 276.5 ± 1.4 K. The south wind was dominant with wind speed mostly less than 3 m/s.
104 The average concentrations of particulate NO_3^-, NH_4^+ and SO_4^{2-} were 39.8 ± 14.7 μg/m^3,
105 27.7 ± 8.6 μg/m^3 and 42.4 ± 16.0 μg/m^3, respectively. The ratios of particulate NO_3^-
106 concentrations to SNA (including sulfate, nitrate and ammonium) were $36.5 \pm 4.0\%$.

2.2 NH_3 emission inventory

108   A comprehensive NH_3 emission inventory of northern China (including the six
109 provinces mentioned above) in December 2015 at a monthly and 1 km × 1 km resolution
110 is developed based our previous studies (Huang et al., 2012;Kang et al., 2016). Here is a
111 brief introduction to our inventory. More detailed descriptions and validation are in our
112 previous studies. Our NH_3 emission inventory is a bottom-up process-based and statistical
113 model which considers a diverse range of sources, including both agricultural (livestock
114 manure and chemical fertilizer) and non-agricultural sectors (e.g., traffic, biomass burning
115 etc.). According to our inventory, the estimated NH_3 emission amount in northern China

116 was 100 kiloton in December 2015. The largest source was livestock waste (57 kiloton,
117 57.0% of the total emissions), following by vehicle (12.2%), chemical industry (8.8%),
118 biomass burning (5.4%), waste disposal (4.0%), synthetic fertilizer applications (2.4%) and
119 other minor sources (9.1%). The proportion of chemical fertilizer is small due to the limited
120 fertilization activity in winter. In the past few years, our inventory has been compared with
121 many studies to prove its reliability. For example, the spatial pattern of NH_3 emissions
122 calculated in our inventory agreed well with the distribution of the NH_3 column
123 concentrations in eastern Asia retrieved from the satellite measurements of Infrared
124 Atmospheric Sounding Interferometer (IASI) (Van Damme et al., 2014). Specially, our
125 estimation of livestock NH_3 emissions in China is comparable to the results of Streets et al.
126 (2003) and Ohara et al. (2007).

127 Another method for estimating NH_3 emissions is the inverse modeling method, which
128 provides top-down emission estimates through optimizing comparisons of model
129 simulations with measurements. For example, Paulot et al. (2014) used the adjoint of a
130 global chemical transport model (GEOS-Chem) and data of NH_4^+ wet deposition fluxes to
131 optimize NH_3 emissions estimation in China. Zhang et al. (2018a) applied TES satellite
132 observations of NH_3 column concentration and GEOS-Chem to provide top-down
133 constraints on NH_3 emissions in China. Their estimates are 10.2 Tg a^{-1} and 11.7 Tg a^{-1}
134 respectively, which are close to our results (9.8 Tg a^{-1}) (Paulot et al., 2014;Zhang et al.,
135 2018a). The accuracy of this method relies on many factors, such as the accuracy of initial
136 conditions, the emission inventories, meteorological inputs, reaction rate constants, and
137 deposition parameters in the chemical transport model. Errors of these parameters could
138 cause biases in the top-down estimation of NH_3 emissions. In addition, measurements of
139 NH_3 or NH_4^+ used in this method, including surface and satellite date, are usually sparse in
140 spatial coverage and have uncertainties, which will also affect the estimation of NH_3
141 emissions.

2.3 ISORROPIA-II and WRF-Chem models

143 The thermodynamic equilibrium model, ISORROPIA-II (Fountoukis and Nenes,
144 2007), being used to determine the phase state and composition of an NH_4^+- SO_4^{2-} - NO_3^- -
145 K^+ - Ca^{2+} - Mg^{2+} - Na^+ - Cl^- - H_2O aerosol system with its corresponding gas components
146 in thermodynamic equilibrium, was used to investigate the response of particulate NO_3^- to
147 NH_3 emission reductions. Using measurements of water-soluble ions, T and RH from
148 PKUERS as inputs, ISORROPIA-II can avoid the inherent uncertainty in estimates of
149 emission inventories, pollutant transport, and chemical transformation. In this study,
150 ISORROPIA-II was run in the "forward mode" and assuming particles are "metastable"
151 with no solid precipitates, which is due to the relatively high RH range observed during
152 this haze event (RH = 60.9 ± 11.4%).

153 We assess the performance of ISORROPIA-II by comparing measured and predicted
154 particulate NO_3^-, NH_4^+ and gaseous HNO_3, NH_3. An error metric, the mean bias (MB), is
155 used to quantify the bias (the description of MB is shown below Figure S1). The predicted
156 particulate NO_3^-, NH_4^+ and NH_3 agree well with the measurements and the value of R^2 are
157 0.99, 0.94 and 0.84, respectively (Figure S1). The MB is only 1.0 μg/m^3, 0.3 μg/m^3 and -
158 1.8 μg/m^3, respectively. However, the model performs poorly on HNO_3, with an R^2 of only
159 0.06 and a MB of -1.0 μg/m^3. This is because particulate NO_3^- is predominantly in the
160 particle phase (the mass ratio of particulate NO_3^- to the total nitric acid (TN = NO_3^- + HNO_3)

was 99.2 ± 1.9%), small errors in predicting particulate NO_3^- are amplified in HNO_3 predicting. Since the MB of HNO_3 is much smaller than the observed particulate NO_3^- (39.8 ± 14.7 μg/m^3) and NH_4^+ (27.7 ± 8.6 μg/m^3), this bias have little influence on simulating the efficiency of particulate NO_3^- reductions.

In the real atmosphere, changes in the level of TA (TA = NH_4^+ + NH_3) can affect the lifetime of TN (Pandis and Seinfeld, 1990). This is because the gaseous HNO_3 has a faster deposition rate in the atmosphere than particulate NO_3^-, and reductions in NH_4^+ may prompt particulate NO_3^- partitioning into the gas phase. In such a case, the concentration of TN would not remain constant but decrease. In order to consider these, we use the Weather Research and Forecast Model coupled Chemistry (WRF-Chem) model (ver. 3.6.1) to investigate the effect of NH_3 emission controls on particulate NO_3^- formation in the regional scale. The simulations were performed for the severe haze event during 6 to 10 December 2015. The modeling domain covered the whole northern China with horizontal resolution of 25 km and 24 vertical layers from surface to 50 hPa. The initial meteorological fields and boundary conditions were taken from the 6 h National Centers for Environmental Prediction (NCEP) global final analysis with a 1° × 1° spatial resolution. The inorganic gas-aerosol equilibrium was predicted by Multicomponent Equilibrium Solver for Aerosols (MESA) in WRF-Chem (Zaveri et al., 2005). The Carbon-Bond Mechanism version Z (CBMZ) photochemical mechanism and Model for Simulating Aerosol Interactions and Chemistry (MOSAIC) aerosol model were used in this study (Fast et al., 2006). Anthropogenic emissions from power plants, industrial sites, residential locations, and vehicles were taken from the Multi-resolution Emission Inventory for China (MEIC; available at www.meicmodel.org).

The performance of WRF-Chem is evaluated by comparing measured and simulated NO_3^-, NH_4^+, SO_4^{2-} and TA. Specifically, the observed and simulated values are, respectively: (1) NO_3^-, 39.8 ± 14.7 μg/m^3 versus 39.1 ± 15.6 μg/m^3; (2) NH_4^+, 27.7 ± 8.6 μg/m^3 versus 26.5 ± 11.7 μg/m^3; (3) SO_4^{2-}, 42.4 ± 16.0 μg/m^3 versus 39.7 ± 20.8 μg/m^3 and (4) TA, 34.6 ± 8.5 μg/m^3 versus 32.1 ± 11.0 μg/m^3. The MB of these four species are -0.7, -1.2, -2.7 and -2.5 μg/m^3, respectively. Simulated particulate NO_3^-, NH_4^+, SO_4^{2-} and TA approximately agreed with the measurements (Figure S2). There are still some simulation biases that may affect the simulation of particulate NO_3^- reductions efficiency. This is discussed in detail in Sect 3.3.

3 Results

3.1 High potential reduction of wintertime NH_3 emissions in northern China

Livestock husbandry accounts for the largest proportion of NH_3 emissions in winter of northern China (approximately 60%), which is mainly caused by the poor manure management. There are three main animal-rearing systems in China: free-range, grazing and intensive. On the one hand, the proportion of intensive livestock husbandry in China is only about 40%, far lower than that of developed countries (Harun and Ogneva-Himmelberger., 2013). As a result, the widespread free-range and grazing animal rearing systems contribute more than half of the total livestock NH_3 emissions due to lacking manure collection and treatment (Kang et al., 2016). On the other hand, there were no relevant regulations about storage of manure for intensive farms in China in the past few

205 decades. This causes most livestock farms also lack necessary measures and facilities for
206 manure collection and storage (Chadwick et al., 2015).

207   Due to the current poor manure management in China, the improved manure
208 management may have great potential for NH_3 emission reductions from livestock
209 husbandry (Wang et al., 2017). The improved manure management mainly includes three
210 phases: in-house handling, storage and land application (Chadwick et al., 2011). For winter,
211 the emission reduction measures mainly focus on in-house handling and storage, since land
212 application mainly occurs in spring and summer. According to previous studies, for in-
213 house handling, regularly washing the floor and using slatted floor or deep litter to replace
214 solid floor could both reduce NH_3 emissions by more than 50% (Groenestein and
215 VanFaassen, 1996;Monteny and Erisman, 1998;Gilhespy et al., 2009;Hou et al., 2015). For
216 storage, covering slurry and manure could reduce NH_3 emissions by about 50%-70%
217 (Balsari. et al., 2006;Petersen et al., 2013;Hou et al., 2015;Wang et al., 2017).

218   Based on the above research results, the livestock NH_3 emission reductions strategies
219 applied in this study include the following steps. Firstly, the proportion of intensive
220 livestock production was raised from 40% to 80% in our NH_3 emission inventory model.
221 In our model, the animals in free-range and grazing animal rearing systems are assumed to
222 live outdoors for half a day, and the improved manure management is only effective for
223 indoor animals. Therefore, increasing the proportion of intensive livestock production is
224 conducive to better manure management (Hristov et al., 2011). Secondly, the ratios of NH_3
225 emission reductions mentioned above were multiplied by NH_3 emission factors in two
226 phases of manure management: 50% reduction at in-house handling and 60% (average
227 value of 50% and 70%) reduction at storage. With these measures, we estimate that the
228 NH_3 emission factors for the livestock in China could be comparable to those in Europe
229 and the USA (shown in Table S1). Meanwhile, our NH_3 emission model predicted that the
230 livestock NH_3 emissions were reduced by 60% (from 57 to 23 kiloton), causing
231 approximately 40% reduction in total NH_3 emissions. Spatially, NH_3 emissions decreased
232 significantly in Hebei, Henan and Shandong, where the livestock NH_3 emissions accounted
233 for a large proportion of the total (shown in Figure S3).

234 3.2. Simulations of NO_3^- reduction due to NH_3 emission controls

235   In the ISORROPIA-II simulation, 40% reduction of TA was used to reflect the effects
236 of reducing NH_3 emissions by 40%. This approach has been used in many previous studies
237 (Blanchard and Hidy, 2003;Vayenas et al., 2005). However, in the real atmosphere, the
238 reductions of NH_3 emission are not always equal to the reductions of TA due to the regional
239 transmission. Their differences are discussed in the WRF-Chem simulation.

240   In this haze event (from 6 to 10 December, 2015), the mean concentration of particulate
241 NO_3^- decreased from 40.8 to 25.7 μg/m^3 (a 37% reduction). In addition, the peak hourly
242 concentration of NO_3^- decreased from 81.9 to 30.7 μg/m^3 (a 63% reduction) (shown in
243 Figure 1). The fundamental thermodynamic processes of TA reductions on decreasing
244 particulate NO_3^- are explained below. Firstly, we found that NH_3 was quite available to
245 react with HNO_3 in the thermodynamic equilibrium system, because NH_3 was 6.6 ± 3.8
246 μg/m^3 while HNO_3 was only 0.4 ± 1.1 μg/m^3. Secondly, almost all of particulate NO_3^-
247 condensed into aerosol phase (the mass ratio of particulate NO_3^- to TN was 99.2 ± 1.9%)
248 under such low temperature conditions (276.5 ± 1.4 K). Thirdly, the NH_3-HNO_3 partial

pressure production (Kp) was as low as about 0.1 ppb^2 (calculated from ISORROPIA-II outputs, depending not only on temperature and RH but also sulfate concentration). The value of K_P would remain constant, if the temperature, RH and sulfate concentration remained unchanged. In general, NH_4NO_3 was not easy to volatilize into gas phase under these circumstances.
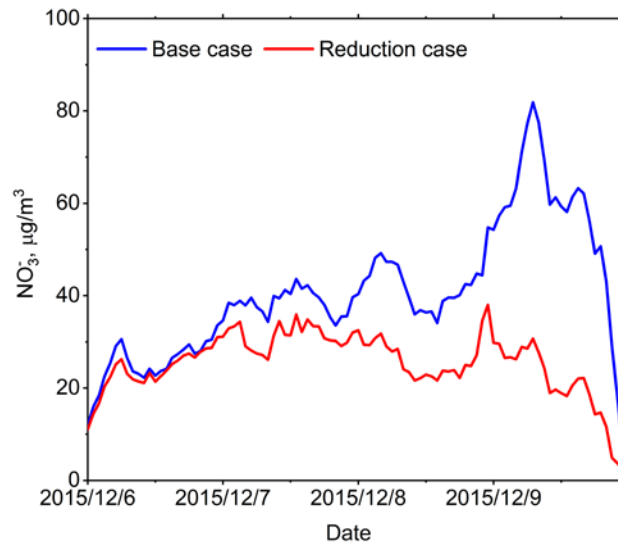

Figure 1. A comparison of particulate nitrate (NO_3^-) between the base (blue line) and emission reductions cases (red line) simulated by the ISORROPIA-II model in this severe haze episode.

When TA was reduced by 40%, the average mass concentration of gaseous NH_3 decreased from 6.6 to 0.01 $\mu g/m^3$ (from 8.8 ppb to 0.05 ppb). In order to keep the value of K_P constant in the thermodynamic equilibrium state, the reductions of NH_3 increased HNO_3, which shifted the particulate NO_3^- partitioning toward the gas phase. Hence, when NH_3 in gas phase was almost completely depleted, HNO_3 increased from 0.4 to 15.5 $\mu g/m^3$ (from 0.1 ppb to 5.6 ppb), leading to a reduction of particulate NO_3^- from 40.8 to 25.7 $\mu g/m^3$ (a 37.0 % reduction). Meanwhile, NH_4^+ also decreased from 27.9 to 20.6 $\mu g/m^3$ and there was almost no change in sulfate level (decreased from 39.7 to 39.3 $\mu g/m^3$), with only trace amount of NH_4HSO_4 produced. This indicated that the reduction of particulate NH_4^+ and NO_3^- was mainly due to the reduction of NH_4NO_3. The sum of particulate NO_3^- and NH_4^+ decreased from 68.7 to 46.3 $\mu g/m^3$ (a 32.6% reduction).

We also conducted WRF-Chem simulations to quantify the impacts of NH_3 emission controls on particulate NO_3^- regionally. A 60% reduction in livestock NH_3 emissions was used as an emission reductions scheme and Figure 2 shows the spatial distribution of particulate NO_3^- under the base case and the emission reductions case. The spatial distribution of particulate NO_3^- was mainly concentrated in most parts of Henan (HN) and Hebei (HB), with the average concentration over 30 $\mu g/m^3$ (included in the black box shown in Figure 2a). The highest particulate NO_3^- concentrations, more than 60 $\mu g/m^3$, were mainly located in central south of Hebei and northern Henan. In the emission

278 reductions case, the mean concentration of particulate NO_3^- decreased from 30.6 to 18.5
279 $\mu g/m^3$ (a 39.4% reduction) in the range of the black box. Meanwhile, the particulate NH_4^+
280 decreased from 16.3 to 11.7 $\mu g/m^3$ (a 28.1% reduction). The sum of particulate NO_3^- and
281 NH_4^+ decreased from 46.9 to 30.2 $\mu g/m^3$ (a 35.6% reduction). Besides, the sulfate
282 concentration slightly changed from 19.7 to 17.6 $\mu g/m^3$, and $PM_{2.5}$ concentration dropped
283 from 143.4 to 125.4 $\mu g/m^3$. The largest reductions in particulate NO_3^- were mainly located
284 in the central north of Henan and central Hebei, where the percentage reduction was
285 generally more than 60% (shown in Figure 2b). In some areas with high particulate NO_3^-
286 concentrations, particulate NO_3^- had been effectively reduced by more than 30 $\mu g/m^3$
287 (shown in Figure 2c). In these regions, severe haze events occurred frequently due to their
288 large emissions of air pollutants, including NH_3 (Wang et al., 2014;Zhao et al., 2017). In
289 addition, TN was reduced by 34.1% (from 31.8 $\mu g/m^3$ to 21.0 $\mu g/m^3$), which was in line
290 with the assumption in Sect 2.3. Correspondingly, TA decreased by 40.7% (from 17.2
291 $\mu g/m^3$ to 10.2 $\mu g/m^3$), very close to the reductions of NH_3 emission (40%). This indicates
292 that it is reasonable to use TA reductions to represent NH_3 emission reductions in the
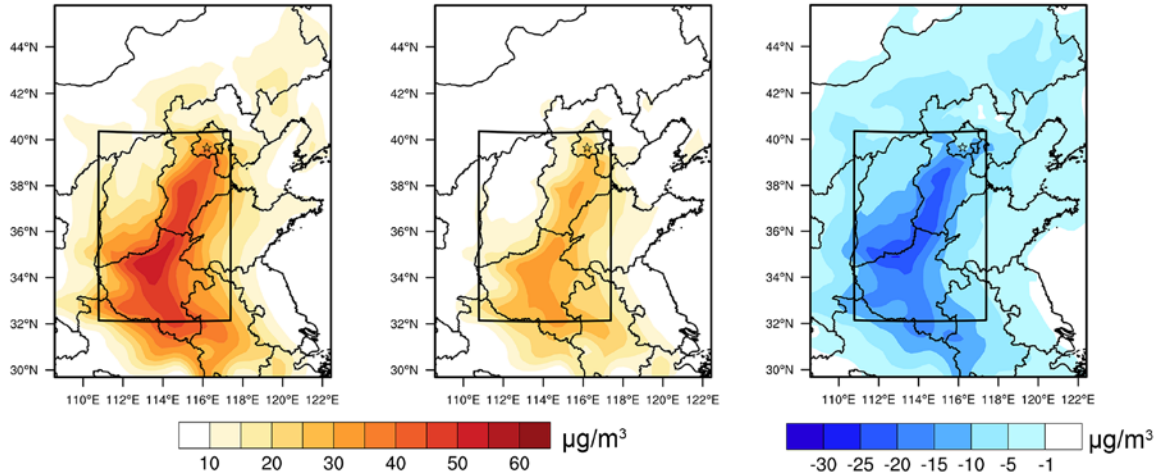293 ISORROPIA-II simulation.

295

296 **Figure 2. (a)** Spatial distribution of particulate NO_3^- concentrations in northern China
297 predicted by WRF-Chem from 6 to 10 December, 2015, for **(a)** the base case, **(b)** the
298 emission reductions case and **(c)** the difference between the base case and the emission
299 reductions case. The scope of this study focuses on the black box, including Beijing (BJ),
300 Tianjin (TJ), Hebei (HB), Shanxi (SX), Shandong (SD) and Henan (HN).

301

302 **3.3 The particulate NO_3^- reduction efficiency during the wintertime**

303 The sensitivity of particulate NO_3^- to NH_3 is often determined by the availability of
304 ambient NH_3, which can be represented by the observable indicator (Seinfeld and Pandis,
305 2006). In this study, we use the observed molar ratio (R) of TA to the sum of sulfate, total
306 chlorine and TN minus Na^+, K^+, Ca^{2+} and Mg^{2+} to represent the availability of ambient
307 NH_3 and predict the sensitivity of the particulate NO_3^- to changes in TN and TA.

308 $$R = \frac{TA}{2SO_4^{2-}+NO_3^-+HNO_3(g)+Cl^-+HCl(g)-2Ca^{2+}-Na^+-K^+-2Mg^{2+}} \quad (1)$$

309   The accuracy of R was examined by constructing the isopleths of particulate NO_3^-
310   concentrations as a function of TN and TA (shown in Figure 3). The NO_3^- concentration
311   was constructed by varying the input concentrations of TA and TN from 0 to 200 μg/m^3 in
312   increments of 10 μg/m^3 independently in ISORROPIA-II, while using the observed average
313   value for the other components. Over a range of temperatures (273–283 K) and RHs (30–
314   90%), the dashed line of R = 1 divides each isopleth into two regions with tiny bias, which
315   indicates that R can be used to qualitatively predict the response of the particulate NO_3^- to
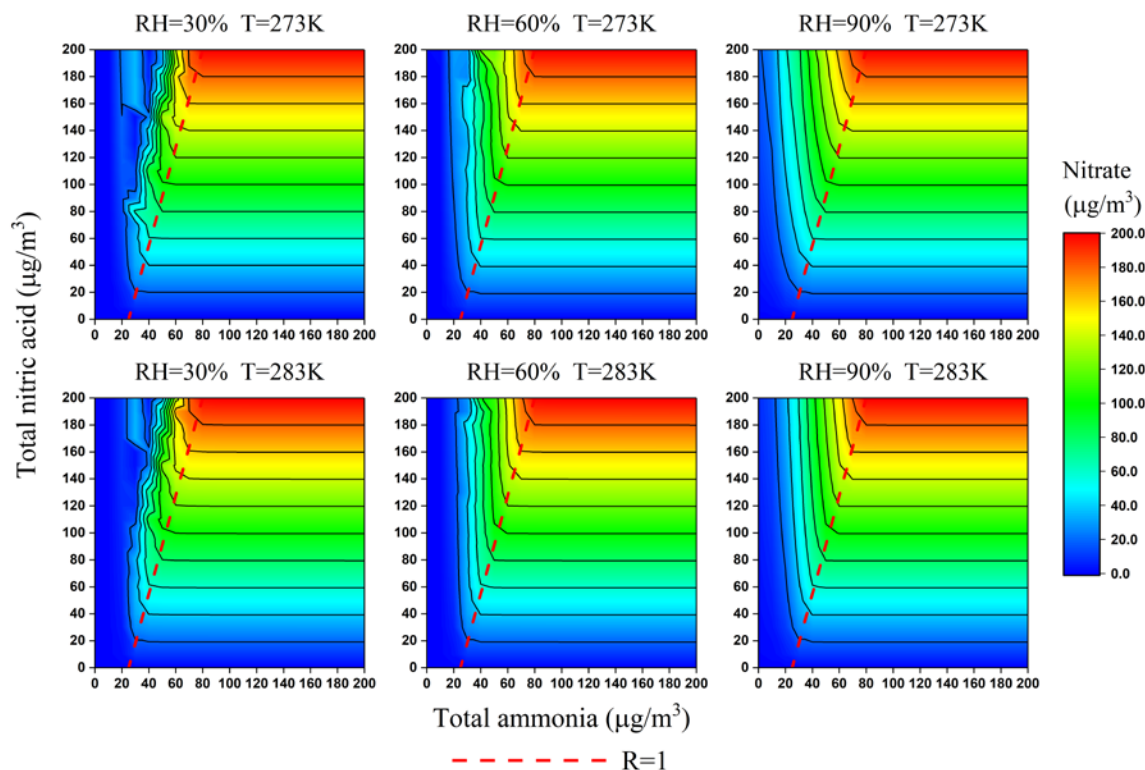316   changes in concentrations of TN and TA.

317

Figure 3. Isopleths of the particulate NO_3^- concentration (μg/m^3) as a function of TN and
TA under average severe haze conditions in winter. The concentration of SO_4^{2-}, Cl^-, K^+,
Ca^{2+}, Na^+, and Mg^{2+} was 60.2, 9.3, 0.56, 0.04, 0.75, and 0.03 μg/m^3, respectively. Values
are averages from all severe hazes during the observation period.

322

323   In the right side of the dashed line (R > 1), particulate NO_3^- formation is HNO_3-limited.
324   The NH_3 is surplus and almost all particulate NO_3^- exists in the aerosol phase. The TA
325   reductions mainly reduce NH_3, with negligible effects on particulate NO_3^-. By contrast,
326   particulate NO_3^- formation is NH_3-limited in the left of the dashed line (R < 1). There is
327   less NH_3 present in the gas phase, and TA reductions could reduce particulate NO_3^-
328   efficiently. For example, when the concentrations of TN and TA are 100 and 50 μg/m^3 (RH
329   = 60 % and T =273 K), the concentration of particulate NO_3^- is about 100 μg/m^3 and the
330   value of R is close to one (typical observational values during the severe haze in this study).
331   In such cases, if TA were reduced by 50% to 25 μg/m^3, the particulate NO_3^- would be
332   significantly reduced from 100 to 20 μg/m^3, an 80% reduction.

333   Under the typical winter conditions in northern China, the value of R was generally
334   greater than one and gradually declining with the increase in SNA concentrations (shown
335   in Figure 4a). When the concentration of SNA is greater than 150 μg/m^3, the values of R
336   become close to and frequently lower than one. This indicated that particulate NO_3^-
337   formation would easily become NH_3-limited under severe haze conditions when NH_3
338   emissions were reduced. In general, particulate NO_3^- will be reduced effectively by a 40%
339   reduction of NH_3 emissions in the condition that the value of R is less than 1.4 (shown in
340   Figure S4). This situation accounts for 68.1% of the entire December (shown in Figure 4b).
341   It should also be noted that the particulate NO_3^- is insensitive to a 40% reduction in NH_3
342   emissions when the value of R is greater than 1.4 (shown in Figure S4). This situation
343   mainly occurs in relatively clean days (the concentration of SNA is less than 75 μg/m^3),
344   accounting for only 31.9% of the entire December (shown in Figure 4a and 4b). Overall,
345   reducing 40% of NH_3 emissions could effectively reduce the levels of particulate NO_3^-
346   under typical severe winter haze conditions in northern China.
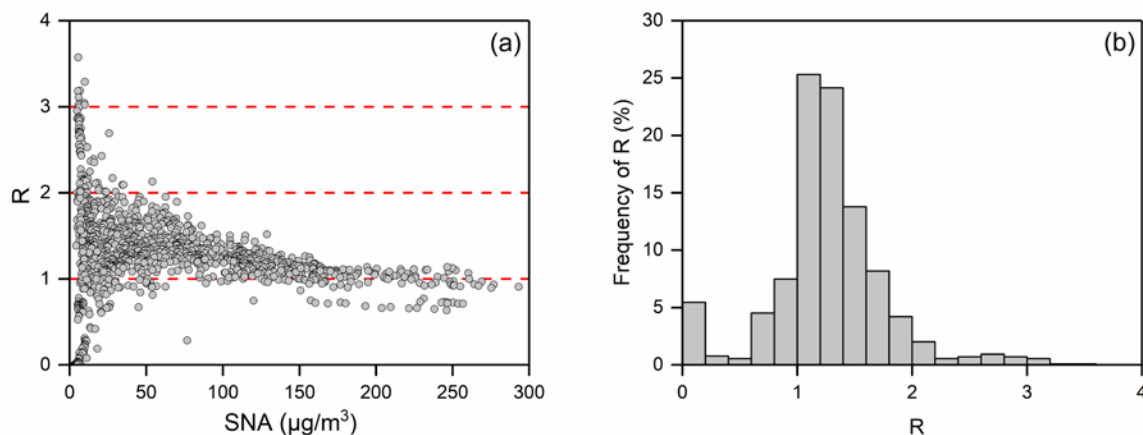

348   **Figure 4.** (a) The observed molar ratio (R) and the concentrations of SNA in PKUERS in
349   December 2015 and December 2016. (b) The frequency of R during the same period.

351   The observed R provides a simple method to rapidly estimate the efficiency of NH_3
352   emission reductions on the particulate NO_3^- reductions, which can avoid the shortage of the
353   air quality model, especially the uncertain estimates of meteorology. However, it also needs
354   to be examined in more detail for specific pollution and meteorological conditions.
355   Therefore, the observed indicator and air quality models should be used in a
356   complementary way to assess the effectiveness of NH_3 emission controls strategies.

357   Based on the above analysis, the influence of WRF-Chem simulation biases on
358   particulate NO_3^- reduction efficiency simulation mainly depends on the simulation bias of
359   R. During the simulation case, the average simulated value of R is 1.3, which is equivalent
360   to the observed value (1.3). Since WRF-Chem has a good estimation of the availability of
361   ambient NH_3, its estimation of the efficiency of particulate NO_3^- reductions is reliable.

362   It is noteworthy that the efficiency of particulate NO_3^- reductions by NH_3 emission
363   controls in northern China during severe winter hazes may be higher than that in the United
364   States and Europe. Compared with our results (40% NH_3 emission reductions lead to about

365   40% particulate NO_3^- reductions), in the United States and Europe, NH_3 emissions often
366   need to be reduced by more than 70% before particulate NO_3^- begin to decrease (Pozzer et
367   al., 2017;Guo et al., 2018a). This is mainly because the strict emission controls of SO_2 and
368   NO_x in these areas lead to a more ammonia-rich environment, which makes particulate
369   NO_3^- insensitive to NH_3 emission reductions.

370

4 Conclusions

372   In this study, we found that during severe winter haze episodes, the particulate NO_3^-
373   formation is NH_3-limited, resulting in its high sensitivity to NH_3 emission reductions.
374   Meanwhile, livestock NH_3 emission controls is a very efficient way to alleviate particulate
375   NO_3^- pollution during severe winter hazes. The estimations showed that the improvements
376   in manure management of livestock husbandry could effectively reduce total NH_3
377   emissions by 40% (from 100 kiloton to 60 kiloton) in winter of northern China. It would
378   lead to a reduction of particulate NO_3^- by about 40% (averagely from 40.8 to 25.7 $\mu g/m^3$)
379   during severe haze conditions.

380   NO_x emission controls could be a more direct and effective way to reduce the
381   particulate NO_3^- than NH_3 emission reductions. However, in northern China, the target of
382   NO_x emission reductions is only about 25% in the 13th Five-Year Plan (2016-2020)
383   (http://www.gov.cn/zhengce/content/2017-01/05/content_5156789.htm). Due to the
384   dominance of free-range animal rearing systems and the lack of emission controls policies,
385   livestock NH_3 emission reductions in China could be practicable. In order to control $PM_{2.5}$
386   pollution more effectively in northern China, measures to improve manure management in
387   livestock urgently need to be implemented.

388

389

396

References

398

399   Backes, A. M., Aulinger, A., Bieser, J., Matthias, V., and Quante, M.: Ammonia emissions
400   in Europe, part II: How ammonia emission abatement strategies affect secondary
401   aerosols, Atmos. Environ., 126, 153-161, 10.1016/j.atmosenv.2015.11.039, 2016.
402   Balsari., P., Dinuccio;, E., and Gioelli;, F.: A low cost solution for ammonia emission
403   abatement from slurry storage, International Congress Series,
404   10.1016/j.ics.2006.02.045, 2006.
405   Bessagnet, B., Beauchamp, M., Guerreiro, C., de Leeuw, F., Tsyro, S., Colette, A., Meleux,
406   F., Rouil, L., Ruyssenaars, P., Sauter, F., Velders, G. J. M., Foltescu, V. L., and van

Aardenne, J.: Can further mitigation of ammonia emissions reduce exceedances of particulate matter air quality standards?, Environ Sci Policy, 44, 149-163, 10.1016/j.envsci.2014.07.011, 2014.

Blanchard, C. L., and Hidy, G. M.: Effects of changes in sulfate, ammonia, and nitric acid on particulate nitrate concentrations in the southeastern United States, J Air Waste Manage, 53, 283-290, Doi 10.1080/10473289.2003.10466152, 2003.

Chadwick, D., Sommer, S. G., Thorman, R., Fangueiro, D., Cardenas, L., Amon, B., and Misselbrook, T.: Manure management: Implications for greenhouse gas emissions, Anim Feed Sci Tech, 166-67, 514-531, 10.1016/j.anifeedsci.2011.04.036, 2011.

Chadwick, D., Jia, W., Tong, Y. A., Yu, G. H., Shen, Q. R., and Chen, Q.: Improving manure nutrient management towards sustainable agricultural intensification in China, Agr Ecosyst Environ, 209, 34-46, 10.1016/j.agee.2015.03.025, 2015.

de Meij, A., Thunis, P., Bessagnet, B., and Cuvelier, C.: The sensitivity of the CHIMERE model to emissions reduction scenarios on air quality in Northern Italy, Atmos. Environ., 43, 1897-1907, 10.1016/j.atmosenv.2008.12.036, 2009.

Fast, J. D., Gustafson, W. I., Easter, R. C., Zaveri, R. A., Barnard, J. C., Chapman, E. G., Grell, G. A., and Peckham, S. E.: Evolution of ozone, particulates, and aerosol direct radiative forcing in the vicinity of Houston using a fully coupled meteorology-chemistry-aerosol model, J. Geophys. Res.-Atmos., 111, 10.1029/2005jd006721, 2006.

Fountoukis, C., and Nenes, A.: ISORROPIA II: a computationally efficient thermodynamic equilibrium model for $K^+–Ca^{2+}–Mg^{2+}–NH_4^+–Na^+–SO_4^{2-}–NO_3^-–Cl^-–H_2O$ aerosols, Atmos. Chem. Phys., 7, 4639-4659, 10.5194/acp-7-4639-2007, 2007.

Fu, X., Wang, S. X., Xing, J., Zhang, X. Y., Wang, T., and Hao, J. M.: Increasing Ammonia Concentrations Reduce the Effectiveness of Particle Pollution Control Achieved via SO_2 and NOx Emissions Reduction in East China, Environ. Sci. Technol. Lett., 4, 221-227, 2017.

Geng, G., Zhang, Q., Tong, D., Li, M., Zheng, Y., Wang, S., and He, K.: Chemical composition of ambient $PM_{2.5}$ over China and relationship to precursor emissions during 2005–2012, Atmos. Chem. Phys., 17, 9187-9203, 10.5194/acp-17-9187-2017, 2017.

Gilhespy, S. L., Webb, J., Chadwick, D. R., Misselbrook, T. H., Kay, R., Camp, V., Retter, A. L., and Bason, A.: Will additional straw bedding in buildings housing cattle and pigs reduce ammonia emissions?, Biosyst Eng, 102, 180-189, 10.1016/j.biosystemseng.2008.10.005, 2009.

Groenestein, C. M., and VanFaassen, H. G.: Volatilization of ammonia, nitrous oxide and nitric oxide in deep-litter systems for fattening pigs, J Agr Eng Res, 65, 269-274, DOI 10.1006/jaer.1996.0100, 1996.

Guo, H., Otjes, R., Schlag, P., Kiendler-Scharr, A., Nenes, A., and Weber, R. J.: Effectiveness of Ammonia Reduction on Control of Fine Particle Nitrate, Atmospheric Chemistry and Physics Discussions, 1-31, 10.5194/acp-2018-378, 2018a.

Guo, H. Y., Otjes, R., Schlag, P., Kiendler-Scharr, A., Nenes, A., and Weber, R. J.: Effectiveness of ammonia reduction on control of fine particle nitrate, Atmos Chem Phys, 18, 12241-12256, 10.5194/acp-18-12241-2018, 2018b.

Harun, S. M. R., and Ogneva-Himmelberger., Y.: Distribution of Industrial Farms in the United States and Socioeconomic, Health, and Environmental Characteristics of Counties, Geography Journal, org/10.1155/2013/385893, 2013.

Hou, Y., Velthof, G. L., and Oenema, O.: Mitigation of ammonia, nitrous oxide and methane emissions from manure management chains: a meta-analysis and integrated assessment, Glob. Change Biol., 21, 1293-1312, 2015.

Hristov, A. N., Hanigan, M., Cole, A., Todd, R., McAllister, T. A., Ndegwa, P. M., and Rotz, A.: Review: Ammonia emissions from dairy farms and beef feedlots, Can J Anim Sci, 91, 1-35, 2011.

Huang, X., Song, Y., Li, M. M., Li, J. F., Huo, Q., Cai, X. H., Zhu, T., Hu, M., and Zhang, H. S.: A high-resolution ammonia emission inventory in China, Glob. Biogeochem. Cycle, 26, 10.1029/2011gb004161, 2012.

Kang, Y. N., Liu, M. X., Song, Y., Huang, X., Yao, H., Cai, X. H., Zhang, H. S., Kang, L., Liu, X. J., Yan, X. Y., He, H., Zhang, Q., Shao, M., and Zhu, T.: High-resolution ammonia emissions inventories in China from 1980 to 2012, Atmos. Chem. Phys., 16, 2043-2058, 10.5194/acp-16-2043-2016, 2016.

Li, C., McLinden, C., Fioletov, V., Krotkov, N., Carn, S., Joiner, J., Streets, D., He, H., Ren, X., Li, Z., and Dickerson, R. R.: India Is Overtaking China as the World's Largest Emitter of Anthropogenic Sulfur Dioxide, Sci Rep, 7, 14304, 10.1038/s41598-017-14639-8, 2017.

Liu, F., Beirle, S., Zhang, Q., van der, A. R., Zheng, B., Tong, D., and He, K.: NOx emission trends over Chinese cities estimated from OMI observations during 2005 to 2015, Atmos Chem Phys, 17, 9261-9275, 10.5194/acp-17-9261-2017, 2017a.

Liu, M. X., Song, Y., Zhou, T., Xu, Z. Y., Yan, C. Q., Zheng, M., Wu, Z. J., Hu, M., Wu, Y. S., and Zhu, T.: Fine particle pH during severe haze episodes in northern China, Geophys. Res. Lett., 44, 5213-5221, 10.1002/2017gl073210, 2017b.

Monteny, G. J., and Erisman, J. W.: Ammonia emission from dairy cow buildings: A review of measurement techniques, influencing factors and possibilities for reduction, Neth J Agr Sci, 46, 225-247, 1998.

Ohara, T., Akimoto, H., Kurokawa, J., Horii, N., Yamaji, K., Yan, X., and Hayasaka, T.: An Asian emission inventory of anthropogenic emission sources for the period 1980-2020, Atmos. Chem. Phys., 7, 4419-4444, DOI 10.5194/acp-7-4419-2007, 2007.

Pandis, S. N., and Seinfeld, J. H.: On the Interaction between Equilibration Processes and Wet or Dry Deposition, Atmos Environ a-Gen, 24, 2313-2327, 10.1016/0960-1686(90)90325-H, 1990.

Paulot, F., Jacob, D. J., Pinder, R. W., Bash, J. O., Travis, K., and Henze, D. K.: Ammonia emissions in the United States, European Union, and China derived by high-resolution inversion of ammonium wet deposition data: Interpretation with a new agricultural emissions inventory (MASAGE_NH$_3$), J. Geophys. Res.-Atmos., 119, 4343-4364, 10.1002/2013jd021130, 2014.

Petersen, S. O., Dorno, N., Lindholst, S., Feilberg, A., and Eriksen, J.: Emissions of CH$_4$, N$_2$O, NH$_3$ and odorants from pig slurry during winter and summer storage, Nutr Cycl Agroecosys, 95, 103-113, 10.1007/s10705-013-9551-3, 2013.

Pinder, R. W., Adams, P. J., and Pandis, S. N.: Ammonia emission controls as a cost-effective strategy for reducing atmospheric particulate matter in the eastern United States, Environ. Sci. Technol., 41, 380-386, 10.1021/es060379a, 2007.

498 Pinder, R. W., Gilliland, A. B., and Dennis, R. L.: Environmental impact of atmospheric
499   NH_3 emissions under present and future conditions in the eastern United States,
500   Geophys. Res. Lett., 35, Artn L1280810.1029/2008gl033732, 2008.
501 Plautz, J.: Piercing the Haze, Science, 361, 1060-1063, 10.1126/science.361.6407.1060,
502   2018.
503 Pozzer, A., Tsimpidi, A. P., Karydis, V. A., de Meij, A., and Lelieveld, J.: Impact of
504   agricultural emission reductions on fine-particulate matter and public health, Atmos.
505   Chem. Phys., 17, 12813-12826, 10.5194/acp-17-12813-2017, 2017.
506 Seinfeld, J. H., and Pandis, S. N.: Atmospheric chemistry and physics : from air pollution
507   to climate change, 2nd ed., Wiley, New York, xxviii, 1202 p. pp., 2006.
508 Streets, D. G., Bond, T. C., Carmichael, G. R., Fernandes, S. D., Fu, Q., He, D., Klimont,
509   Z., Nelson, S. M., Tsai, N. Y., Wang, M. Q., Woo, J. H., and Yarber, K. F.: An
510   inventory of gaseous and primary aerosol emissions in Asia in the year 2000, J.
511   Geophys. Res.-Atmos., 108, Artn 880910.1029/2002jd003093, 2003.
512 Tan, T. Y., Hu, M., Li, M. R., Guo, Q. F., Wu, Y. S., Fang, X., Gu, F. T., Wang, Y., and
513   Wu, Z. J.: New insight into $PM_{2.5}$ pollution patterns in Beijing based on one-year
514   measurement of chemical compositions, Sci. Total Environ., 621, 734-743,
515   10.1016/j.scitotenv.2017.11.208, 2018.
516 Tsimpidi, A. P., Karydis, V. A., and Pandis, S. N.: Response of inorganic fine particulate
517   matter to emission changes of sulfur dioxide and ammonia: The eastern United States
518   as a case study, J Air Waste Manage, 57, 1489-1498, 10.3155/1047-3289.57.12.1489,
519   2007.
520 Van Damme, M., Clarisse, L., Heald, C. L., Hurtmans, D., Ngadi, Y., Clerbaux, C., Dolman,
521   A. J., Erisman, J. W., and Coheur, P. F.: Global distributions, time series and error
522   characterization of atmospheric ammonia (NH_3) from IASI satellite observations,
523   Atmos. Chem. Phys., 14, 2905-2922, 10.5194/acp-14-2905-2014, 2014.
524 Vayenas, D. V., Takahama, S., Davidson, C. I., and Pandis, S. N.: Simulation of the
525   thermodynamics and removal processes in the sulfate-ammonia-nitric acid system
526   during winter: Implications for $PM_{2.5}$ control strategies, J. Geophys. Res.-Atmos.,
527   110, Artn D07s1410.1029/2004jd005038, 2005.
528 Wang, L. T., Wei, Z., Yang, J., Zhang, Y., Zhang, F. F., Su, J., Meng, C. C., and Zhang,
529   Q.: The 2013 severe haze over southern Hebei, China: model evaluation, source
530   apportionment, and policy implications, Atmos. Chem. Phys., 14, 3151-3173,
531   10.5194/acp-14-3151-2014, 2014.
532 Wang, Y., Dong, H. M., Zhu, Z. P., Gerber, P. J., Xin, H. W., Smith, P., Opio, C., Steinfeld,
533   H., and Chadwick, D.: Mitigating Greenhouse Gas and Ammonia Emissions from
534   Swine Manure Management: A System Analysis, Environ. Sci. Technol., 51, 4503-
535   4511, 2017.
536 Wu, Y. Y., Gu, B. J., Erisman, J. W., Reis, S., Fang, Y. Y., Lu, X. H., and Zhang, X. M.:
537     $PM_{2.5}$ pollution is substantially affected by ammonia emissions in China, Environ.
538   Pollut., 218, 86-94, 10.1016/j.envpol.2016.08.027, 2016.
539 Zaveri, R. A., Easter, R. C., and Peters, L. K.: A computationally efficient multicomponent
540   equilibrium solver for aerosols (MESA), J. Geophys. Res.-Atmos., 110,
541   10.1029/2004jd005618, 2005.
542 Zhang, L., Chen, Y. F., Zhao, Y. H., Henze, D. K., Zhu, L. Y., Song, Y., Paulot, F., Liu,
543   X. J., Pan, Y. P., Lin, Y., and Huang, B. X.: Agricultural ammonia emissions in China:

544   reconciling bottom-up and top-down estimates, Atmos. Chem. Phys., 18, 339-355,
545   10.5194/acp-18-339-2018, 2018a.

546 Zhang, R., Sun, X. S., Shi, A. J., Huang, Y. H., Yan, J., Nie, T., Yan, X., and Li, X.:
547   Secondary inorganic aerosols formation during haze episodes at an urban site in
548   Beijing, China, Atmos. Environ., 177, 275-282, 10.1016/j.atmosenv.2017.12.031,
549   2018b.

550 Zhang, X. Y., Wang, J. Z., Wang, Y. Q., Liu, H. L., Sun, J. Y., and Zhang, Y. M.: Changes
551   in chemical components of aerosol particles in different haze regions in China from
552   2006 to 2013 and contribution of meteorological factors, Atmos. Chem. Phys., 15,
553   12935-12952, 10.5194/acp-15-12935-2015, 2015.

554 Zhao, B., Wu, W. J., Wang, S. X., Xing, J., Chang, X., Liou, K. N., Jiang, J. H., Gu, Y.,
555   Jang, C., Fu, J. S., Zhu, Y., Wang, J. D., Lin, Y., and Hao, J. M.: A modeling study
556   of the nonlinear response of fine particles to air pollutant emissions in the Beijing-
557   Tianjin-Hebei region, Atmos. Chem. Phys., 17, 12031-12050, 10.5194/acp-17-
558   12031-2017, 2017.

559 Zheng, G. J., Duan, F. K., Ma, Y. L., Zhang, Q., Huang, T., Kimoto, T., Cheng, Y. F., Su,
560   H., and He, K. B.: Episode-Based Evolution Pattern Analysis of Haze Pollution:
561   Method Development and Results from Beijing, China, Environ. Sci. Technol., 50,
562   4632-4641, 10.1021/acs.est.5b05593, 2016.

563